Discrimination of maleic hydrazide polymorphs using terahertz spectroscopy and density functional theory*

ZHENG Zhuanping, ZHAO Shuaiyu, LIU Yuhang, and GONG Jiamin**

School of Electronic Engineering, Xi'an University of Posts & Telecommunication, Xi'an 710121, China

(Received 2 December 2022; Revised 3 March 2023)

The terahertz (THz) absorptions of maleic hydrazide polymorphs (MH2 and MH3) have been measured utilizing terahertz time-domain spectroscopy (THz-TDS). MH2 and MH3 have displayed totally different THz absorption features compared to their basically identical infrared spectral peaks. Experimental THz spectrum of MH2 showed six distinct absorption features while MH3 demonstrated five characteristic absorption peaks in the range of 10—160 cm^{-1}. Spectral interpretation has been carried out in the framework of density functional theory (DFT) using periodic unit cell models. The simulation yields a good quality with respect to the measured features. Further analysis into the mode of vibration showed that the low-frequency THz spectral features (<112 cm^{-1}) are contributed by intermolecular interactions mediated by in-plane/out-of-plane collective vibrations. The varied intermolecular interactions and crystal habits are the primarily reason for the THz spectral differences of MH2 and MH3.

Document code: A **Article ID:** 1673-1905(2023)08-0493-5

DOI https://doi.org/10.1007/s11801-023-2205-z

With the stable terahertz (THz) source becoming a conventional technology, more and more researches have been conducted on THz waves[1,2]. Terahertz time-domain spectroscopy (THz-TDS), regarded as a well-established technology, is now popularly used in fundamental research and industrial applications[3,4]. With the frequency covering in the range of 0.1—3 THz, THz-TDS has become a promising tool to study molecular new aspects of weak noncovalent intermolecular bonds, such as hydrogen bonds and van der Waals forces[5]. Compared to the sensitive to localized atomic motions in mid-infrared spectroscopy, THz spectroscopy prefers to probe molecular system in a globe sense where all atoms are in the entire molecule. The fact that THz absorptions are not only sensitive to molecule but also for its environment leads the investigation and identification of polymorph pharmaceutical more efficient[6-8]. For instance, different polymorphs have been given rise to different THz absorption spectra[8].

However, the measured THz spectrum is only of great value when the peaks assignment is successfully made. Isolated-molecule theory is reported failure to interpret solid-state THz measurement due to the absence of environmental interactions[9]. The interpretation of solid-state THz measurements only can be accomplished through solid-state theory which considers the crystal cell interactions. The simulation using periodic unit cell models remarkably improves the ability for THz spectral reproduction, leading the physical nature of these low-frequency vibrations to be revealed possibly[10]. Since polymorphs basically share the same molecular structure, it is a crucial task to understand their characteristic THz spectra.

Maleic hydrazide (1,2-dihydropyridazine-3,6-dione, MH), a very popular growth inhibitor used in agriculture, was firstly discovered by CRADWICK[11]. Researchers have shown great interest in its structure and spectra because MH can act as a pyrimidine analogue forming base pairs with adenine. The crystal structure of maleic hydrazide polymorphs (MH1) was reported in 1975[12], the other polymorphs of MH2 and MH3 were predicted later[13,14]. HOFMANN et al[15] theoretically studied the structures of its different tautomer, in which the most stable form of molecular structure in gas state and in solution is shown. MORZYK-OCIEPA[16] reported the infrared spectra of MH and its deuterated derivative. QU et al[17] shown the measured THz spectrum of MH. The low-frequency THz spectra of MH polymorphs have been previously reported in the range of 10—70 cm^{-1} by our group[18]. However, the broad THz spectra of polymorph which is regarded as crucial information in polymorphs chemical function analyses are not investigated yet.

Thus in this paper, we measured the THz spectra and infrared (IR) spectra of MH2 and MH3 using THz-TDS and Fourier transform infrared spectrometer (FT-IR). Unique THz fingerprint spectra of these two polymorphs were obtained compared to their almost the same IR

* This work has been supported by the National Natural Science Foundation for Young Scientists of China (No.11604263).

** E-mail: zhengzhuanping@xupt.edu.cn

absorption spectra. Solid-state density functional theory (DFT) was performed to interpret the observed THz spectra. According to the spectral reproduction, a complete peak assignment of MH2 and MH3 was reported. The differences in the sources of THz absorption peaks were also discussed. In addition, the X-ray diffraction spectra of MH2 and MH3 were also presented to verify the rationality of our research.

The THz spectra were measured using TAS7400TS (Advantest Corporation) with the frequency resolution of 0.26 cm^{-1}. These instruments use a photoconductive antenna system to generate and detect THz radiation, which is excited by femtosecond pulses at 800 nm and 1 550 nm, respectively.

Experimentally, the mid-infrared (MIR) spectrum was measured at 2 cm^{-1} resolution on a VERTEX 70 spectrometer (Bruker Optics Inc.) equipped with a Globar source, a KBr beam splitter, and a DLaTGS Bolometer detector.

MH2 and MH3 were acquired from Hangzhou SoliPharma. The samples were of analytical grade (>99%) and used without further purification. The sample was first crushed into fine powder using mortar and pestle to minimize the particle scattering. Then, it was compressed into thick a pellet containing 2% MH2 (MH3) and 98% potassium bromide to get the IR spectrum, pellets using mixture (sample: PE) to get THz spectrum in the range of 10—160 cm^{-1}.

The solid-state calculations utilizing Perdew-Burke-Ernzerhof (PBE) exchange-correlation functional and Norm-conserving Troullier-Martins pseudopotentials are performed to predict the spectra of MH2 and MH3 in crystal[19]. The vibrational frequency can be obtained from the second order derivative of the Kohn-Sham energy with respect to atomic displacements.

$$\sum_{i,\beta}\frac{1}{(M_iM_{i'})^{1/2}}\frac{\partial^2 E}{\partial q_{i\alpha}\partial q_{j\beta}}e(j\beta)=M_i\omega^2 e(i\alpha), \qquad (1)$$

where $q_{i\alpha}$ is a Cartesian coordinate of a system with N atoms, so that $1<i<3N$, M_i is the mass of atom i, $e(j\beta)$ are atomic displacement eigenvectors, E is the total energy, and ω is the vibrational frequency. The total energy was converged to 10^{-8} eV/atom and the maximum forces between atoms were less than 10^{-5} eV/Å for geometry optimizations. A plane wave cutoff energy was used at 1 400 eV.

The simulations of MH2 and MH3 were performed based on crystal cell parameters taken from Refs.[13,14]: $P2_1/c$ (Z=4), a=6.891 Å, b=9.674 Å, c=6.946 Å, α, γ=90.0°, β=100.07°; $P2_1/n$ (Z=4), a=6.607 Å, b=9.07 Å, c=10.539 Å, α, γ=90.0°, β=104.0°. The molecular structure and molecular packing of MH2 (MH3) has been presented in Fig.1. The hydrogen bonds are indicated by the dashed green lines.

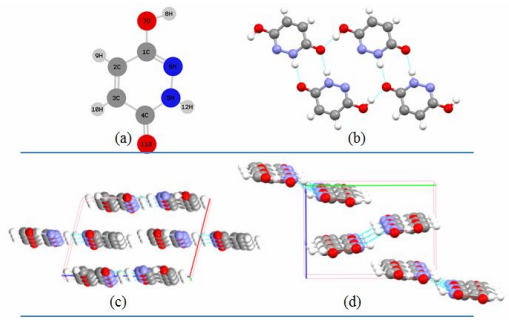

Fig.1 (a) Molecular structure of MH2 (MH3); (b) Molecular packing of the pairs of hydrogen bond chains in MH2 and MH3; (c) Crystal packing of MH2; (d) Crystal packing of MH3

The room temperature THz spectra of MH2 are given in Fig.2 (in green line). MH2 produced a THz spectrum with absorptions located at 12.8 cm^{-1}, 47.2 cm^{-1} and 58.1 cm^{-1} in the range of 10—70 cm^{-1}[18]. As the sample is gradually diluted, the absorption peaks in high-frequency begins to appear, lying at 89.6 cm^{-1}, 122.6 cm^{-1} and 149.6 cm^{-1}. In the measurement, six absorption peaks of MH2 are observed in the range of 10—160 cm^{-1}.

The room temperature THz spectra of MH3 were presented in Fig.2 (in orange line). MH3 exhibits two absorption peaks in the range of 10—70 cm^{-1}, lying at 25.2 cm^{-1} and 61.4 cm^{-1}[18]. As the sample is gradually diluted, the strong absorption peaks in high-frequency begin to appear, lying at 102.9 cm^{-1}, 112.0 cm^{-1} and 140.2 cm^{-1}. According to the spectral comparison between MH2 and MH3, it is clear that these two polymorphs present different THz finger-printing spectral peaks. This result indicates that the THz-TDS can be used for distinguishing between MH2 and MH3.

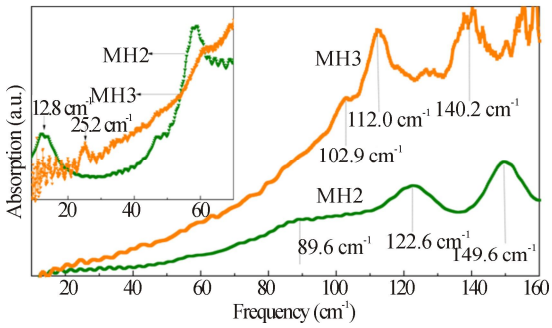

Fig.2 Experimental THz spectra of MH2 and MH3 in 10—160 cm^{-1} region

Fig.3 shows the IR spectra of MH2 and MH3. It can be observed that the IR absorption peaks of MH2 and MH3 are nearly identical in terms of peak positions in the range of 400—4 000 cm^{-1}. It is difficult to be distinguished from each other. These two polymorphs shared the same strong absorption and representative features, such as 517 cm^{-1}, 817 cm^{-1}, 1 005 cm^{-1}, 1 275 cm^{-1},

1 413 cm^{-1}, 1 544 cm^{-1}, 2 500 cm^{-1} and 3 000 cm^{-1}. This is primarily due to that MH2 shared the same molecular structure with MH3, and MH2 exhibits the same scheme of molecular association into hydrogen-bonded ribbons as in MH3 (see Fig.1(b)). These experimental results indicate that MH2 and MH3 are difficult to be identified by their IR spectra. Fortunately, these two polymorphs can be distinguished by their THz absorption peaks at 12.8 cm^{-1} (MH2) and 25.2 cm^{-1} (MH3) in high concentration, identified by the aid of 140.2 cm^{-1} and 149.6 cm^{-1} in low concentration which demonstrates THz-TDS is a promising tool for the characterization of polymorphs.

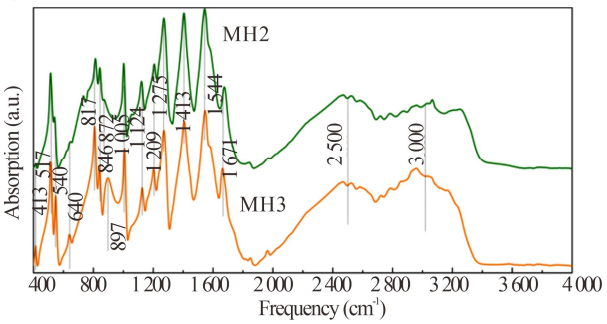

Fig.3 Experimental IR spectra of MH2 and MH3

To analyze the observed THz spectra, DFT calculation is performed on MH2 and MH3. The frequency of each normal mode was calculated within the harmonic approximation at the optimized geometry. Because full optimization of geometry reproduces the crystal structure at absolute zero temperature, the frequency data calculated at the fully optimized geometry are inadequate for comparison with the low-temperature THz spectrum[21]. Thus the geometries in our work were optimized using in the fixed cell for the room-temperature (295 K) crystallographic data.

The experimental spectrum and calculated vibrational modes of MH2 are given in Fig.4. Assignment of the seven IR-active vibrational modes comprising the experimental spectrum is based on the most significant contributor to the vibrational-mode character. Tab.1 lists a description of each mode. According to the reasonable agreement between experimental and calculated data, the assignment of peaks is as following. The features at 12.8 cm^{-1}, 47.2 cm^{-1} and 89.6 cm^{-1} are primarily caused by out-plane rotations. The feature at 58.1 cm^{-1} is mainly dominated by intermolecular vibration due to in-plane rotation. The out-plane bending of CH groups are likely contributed to the peak located at 122.6 cm^{-1}, the intramolecular bending of hydrogen bonds of N-H···O and O-H···O are the mainly reason of the absorption peak of 149.6 cm^{-1}.

The solid-state optical modes of MH3 are compared to the experimental results in Fig.5. Six modes are obtained in MH3 simulation. According to the comparison between experiment and calculation, assignment of peaks is as following. The absorption peaks near 25.2 cm^{-1} and 102.9 cm^{-1} are due to in-plane intermolecular rotation. The peak at 61.4 cm^{-1} is mainly dominated by out-plane intermolecular rotation. The absorption features at 112 cm^{-1} and 140.2 cm^{-1} are mainly contributed by intramolecular vibrations. Tab.1 provides the details assignment.

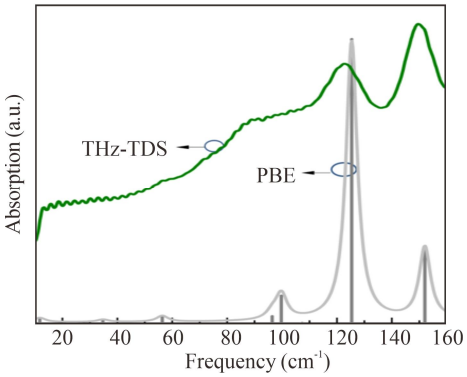

Fig.4 Experimental spectrum and calculated result of MH2 in the range of 10—160 cm^{-1} region

Tab.1 Calculated and experimental THz spectral data of MH2 and MH3 (cm^{-1})

Experiment	Calculation	
MH2	Modes	Assignment
12.8	11.8 (1.15)	out-plane intermolecular rotation along c axis
47.2	34.8 (0.65)	
58.1	56.4 (1.56)	in-plane intermolecular rotations along b axis
89.6	96.4 (1.72)	out-plane intermolecular vibrations along c axis
	99.7 (6.76)	
122.6	125.4 (42.8)	out-plane bending of C-H
149.6	152.0 (18.8)	the butterfly bending of hydrogen bonds
MH3	Modes	Assignment
25.2	25.8 (0.07)	in-plane intermolecular rotation along a axis
	27.0 (0.18)	
61.4	62.4 (0.35)	out-plane intermolecular vibrations along a axis
102.9	102.6 (9.88)	
112.0	111.2 (18.6)	out-plane bending of C-H
140.2	149.1 (2.3)	the butterfly bending between hydrogen bonds and C-H

● Infrared intensities (km/mol) are shown in parentheses.

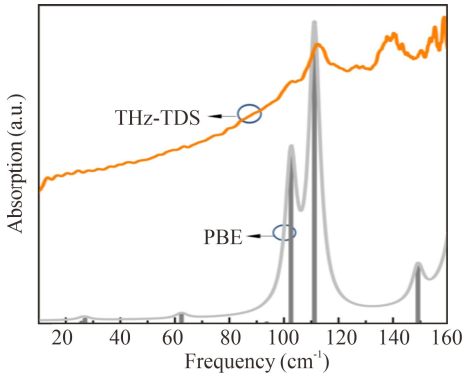

Fig.5 Experimental spectrum and calculated result of MH3 in the range of 10—160 cm^{-1} region

Further analysis into the mode of vibration shows that the features of MH2 at 149.6 cm^{-1} comes from the bending of N-H···O and O-H···O with the contribution of N-H···O more. The feature located at 122.6 cm^{-1} is mainly contributed by the bending of C2-H9 and C3-H10 along with a bit contribution of benzene ring torsion. The observed feature at 140.2 cm^{-1} (MH3) is caused by the torsions between hydrogen bonds and C-H group, in which the hydrogen bonds contribute more. The feature located at 112.0 cm^{-1} is also primarily contributed by C3-H10 and C2-H9 bending but with the contribution of C3-H10 more. Besides, it is found that the peaks of 149.6 cm^{-1} and 140.2 cm^{-1} are affected by the moderate hydrogen bonds of N-H···O and O-H···O, and the peaks of 122.6 cm^{-1} and 112.0 cm^{-1} are influenced by the weak hydrogen bond of C2-H9···N and C2-H9···O[22]. This fact implies that THz spectra (>112 cm^{-1}) are contributed by the combination of inter- and intra-molecular forces but with the contribution of intramolecular vibrations more. Besides, these discussion results also indicate that the high-frequency THz absorption peak is more resulted from the motions of vibration and hydrogen bond bending, and the low-frequency THz absorption peak mainly comes from rotation and translation motions.

Tab.1 lists the assignment of MH2 and MH3. It is obvious that the origins of their measured THz spectra are totally different. This is possibly due to that the arrangements of their aggregates and the details of their supramolecular conformations of MH2 and MH3 are different (see Fig.1(c) and (d)). Their same hydrogen-bonded supramolecular aggregates organize into different lattices of different symmetries, which can induce different molecular forces to satisfy the close-packing condition. The varied intermolecular interactions and crystal habits may lead to the different optical properties of MH2 and MH3. It is noted that the discrepancy between experiment and calculation still exists. Such as the mode at 34.8 cm^{-1}, which is calculated in a region where absorption peak is observed at 47.2 cm^{-1}. This is possible that the total energy of MH2 at this mode is underestimated by the DFT calculations. Besides, the intensity of predicted mode at 125.4 cm^{-1} and 111.2 cm^{-1} are so much high which is possible due to that the change in the dipole moment under atomic displacement at this mode is overestimated. This phenomenon can be modified by using large cutoff energy and smaller separation of k-points in simulation[21]. Besides, small differential IR absorption peaks for MH2 and MH3 are also observed, 731 cm^{-1} and 872 cm^{-1} for MH2, 898 cm^{-1} for MH3. These spectral differences are deduced partly contributed by the noncovalent bonds, especially for the hydrogen bonds, such as N-H···O and O-H···O.

In addition, the X-ray diffraction spectra of MH2 and MH3 were presented in Fig.6, in order to verify the purity of these two polymorphs. In comparison, the XRD spectra match with the data in Refs.[13, 14]. MH2 and MH3 are monoclinic crystals, MH2 is $P21/c$ symmetry, and MH3 is $P21/n$ symmetry, which verifies the rationality of our research.

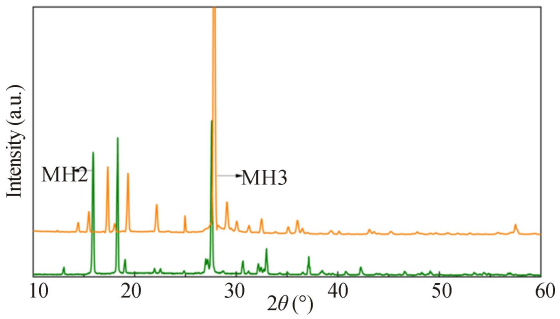

Fig.6 Experimental X-ray diffraction spectra of MH2 and MH3

In this work, the distinct absorption peaks of MH2 and MH3 ranging from 10 cm^{-1} to 160 cm^{-1} are measured. MH2 and MH3 shows different THz absorption features compared to their basically identical infrared spectral peaks. Based on their unique THz spectral feature, MH2 and MH3 polymorphs can be successfully distinguished by THz-TDS. Solid-sate DFT is utilized for the simulations to assign the THz spectra for MH2 and MH3. By carrying out crystal simulations, it is found that the measured features (<112 cm^{-1}) are mainly dominated by intermolecular vibrations. The remaining features are contributed by the combination of inter- and intra-molecular forces with the contribution of intramolecular vibrations more. The THz spectral differences between MH2 and MH3 are primarily caused by their different molecular interactions which are used to satisfy close-packing condition in different lattices of different symmetries. These understanding of the origin of THz spectra in crystalline solids can hold great promise for the polymorphs identification and their chemical function analyses in industry.

Ethics declarations

Conflicts of interest

The authors declare no conflict of interest.

References

[1] MA Y, HUANG H, HAO S, et al. Insights into the water status in hydrous minerals using terahertz time-domain spectroscopy[J]. Scientific reports, 2019, 9(1): 9265.

[2] TENG Y. 120 GHz on-chip multi-mode wideband dielectric resonator antennas for THz applications[J]. Optoelectronics letters, 2020, 16(3): 166-170.

[3] PECCIANTI M, FASTAMPA R, CONTE A M, et al. Terahertz absorption by cellulose: application to ancient paper artifacts[J]. Physical review applied, 2017, 7(6): 064019.

[4] SHEN Y C, YANG X Y, ZHANG Z J. Broadband terahertz time-domain spectroscopy and fast FMCW imaging:

principle and applications[J]. Chinese physics B, 2020, 29(7)：078705.

[5] ZHU Z, BIAN Y, ZHANG X, et al. Terahertz spectroscopy of temperature-induced transformation between glutamic acid, pyroglutamic acid and racemic pyroglutamic acid[J]. Spectrochimica acta part A：molecular and biomolecular spectroscopy, 2022, 275：121150.

[6] BIAN Y, ZHANG X, ZHU Z, et al. Vibrational modes optimization and terahertz time-domain spectroscopy of L-Lysine and L-Lysine hydrate[J]. Journal of molecular structure, 2021, 1232：129952.

[7] WANG P, ZHAO J, ZHANG Y, et al. The fingerprints of nifedipine/isonicotinamide cocrystal polymorph studied by terahertz time-domain spectroscopy[J]. International journal of pharmaceutics, 2022, 620：121759.

[8] DAVIS M P, KORTER T M. Low-frequency vibrational spectroscopy and quantum mechanical simulations of the crystalline polymorphs of the antiviral drug ribavirin[J]. Molecular pharmaceutics, 2022, 19(9)：3385-3393.

[9] ZHENG Z P, LI A D, LI C Y, et al. Terahertz time-domain spectral study of paracetamol[J]. Spectroscopy and spectral analysis, 2021, 41(12)：3660-3664.

[10] ZHANG B, LI S, WANG C, et al. Terahertz spectroscopic investigation of gallic acid and its monohydrate[J]. Spectrochimica acta part A：molecular and biomolecular spectroscopy, 2018, 190：40-46.

[11] CRADWICK P D. On the calculation of one-dimensional X-ray scattering from interstratified material[J]. Clay minerals, 1975, 10(5)：347-356.

[12] CRADWICK P D. Crystal structure of the growth inhibitor,'maleic hydrazide'(1, 2-dihydropyridazine-3, 6-dione)[J]. Journal of the chemical society, perkin transactions 2, 1976, (12)：1386-1389.

[13] KATRUSIAK A. A new polymorph of maleic hydrazide[J]. Acta crystallographica section C：crystal structure communications, 1993, 49(1)：36-39.

[14] KATRUSIAK A. Polymorphism of maleic hydrazide. I[J]. Acta crystallographica section B：structural science, 2001, 57(5)：697-704.

[15] HOFMANN H J, CIMIRAGLIA R, TOMASI J, et al. Structure and tautomerism of maleic hydrazide[J]. Journal of molecular structure：theochem, 1991, 227：321-326.

[16] MORZYK-OCIEPA B. X-ray crystal structure and vibrational spectra of hydrazides and their metal complexes. Part I. Catena-poly [di-μ-aqua-(μ-maleic hydrazidato-O) sodium] hydrate[J]. Journal of molecular structure, 2007, 833(1-3)：121-132.

[17] QU F, PAN Y, LIN L, et al. Experimental and theoretical study on terahertz absorption characteristics and spectral de-noising of three plant growth regulators[J]. Journal of infrared, millimeter, and terahertz waves, 2018, 39(10)：1015-1027.

[18] ZHENG Z P, LI A D, DONG J, et al. Terahertz spectroscopic investigation of maleic hydrazide polymorphs[J]. Spectroscopy and spectral analysis, 2022, 42(04)：1104-1108.

[19] PERDEW J P, BURKE K, ERNZERH M. Generalized gradient approximation made simple[J]. Physical review letters, 1996, 77(18)：3865.

[20] TROULLIER N, MARTINS J L. Efficient pseudopotentials for plane-wave calculations[J]. Physical review B, 1991, 43(3)：1993.

[21] TAKAHASHI M, OKAMURA N, FAN X, et al. Temperature dependence in the terahertz spectrum of nicotinamide：anharmonicity and hydrogen-bonded network[J]. The journal of physical chemistry A, 2017, 121(13)：2558-2564.

[22] STEINER T. The hydrogen bond in the solid state[J]. Angewandte chemie international edition, 2002, 41(1)：48-76.